



Optimization of ADMET Properties Prediction for Remdesivir, Favipiravir, and their Metabolites Elimination Profiles

Anita Purnamayanti^{1,2}  

Suharjono^{3*}  

Mahardian Rahmadi³  

¹ Doctoral Program in Pharmaceutical Sciences, Universitas Airlangga, Surabaya 60115, East Java, Indonesia

² Department of Clinical Pharmacy, Universitas Surabaya, Surabaya, East Java, Indonesia

³ Department of Pharmacy Practices, Universitas Airlangga, Surabaya, East Java, Indonesia

*email: suharjono@ff.unair.ac.id; phone: +628121733877

Keywords:

ADMET
COVID-19
Favipiravir
Pharmacokinetics
Remdesivir

Abstract

In silico methods have become crucial for the rapid preliminary assessment of drug compound absorption, distribution, metabolism, excretion, and toxicity (ADMET) properties, particularly for vital antivirals such as remdesivir and favipiravir, early in the drug development process. This study aimed to predict the pharmacokinetic profiles of remdesivir, favipiravir, and their respective metabolites, explicitly focusing on their interactions within the unique anatomy and physiology of human elimination organs. Compound summaries from PubChem were computationally analyzed using the pkCSM, ProTox-II, and ADMETLab 3.0 platforms. These predictions were then critically evaluated in the context of established hepatic and renal elimination mechanisms. Favipiravir and its metabolites generally exhibited a favorable ADMET profile, characterized by good oral absorption, wide distribution, efficient metabolism, and rapid excretion, albeit with a slight potential for blood-brain barrier penetration. In contrast, remdesivir, its nucleotide metabolite, and favipiravir showed the highest predicted likelihood of inducing hepatotoxicity. Concerning renal toxicity, remdesivir, remdesivir monophosphate, and the active triphosphate forms of both remdesivir and favipiravir presented a notable risk. This elevated renal risk was primarily attributed to their predicted low renal clearances, potentially resulting from insufficient penetration across the negatively charged glomerular filtration barrier. In conclusion, favipiravir and its metabolites demonstrated a more desirable ADMET profile than remdesivir. These preliminary findings suggest a differential safety and pharmacokinetic landscape between the two antiviral agents. Future research should prioritize leveraging advanced AI-based ADMET platforms to simulate complex human organ functions more accurately, refining these predictive models, and guiding subsequent *in vivo* investigations.

Received: October 18th, 2024

1st Revised: August 20th, 2025

2nd Revised: November 6th, 2025

Accepted: December 10th, 2025

Published: March 30th, 2026



© 2026 Anita Purnamayanti, Suharjono, Mahardian Rahmadi. Published by Institute for Research and Community Services Universitas Muhammadiyah Palangkaraya. This is an Open Access article under the CC-BY-SA License (<http://creativecommons.org/licenses/by-sa/4.0/>). DOI: <https://doi.org/10.33084/bjop.v9i1.8464>

INTRODUCTION

Coronavirus disease 2019 (COVID-19), which progressed through multiple devastating global waves, established a defining long-term pandemic crisis of this century. Within the evolving landscape of COVID-19 therapeutics, favipiravir (FPV) and remdesivir (RDV) were initially evaluated in phase-3 clinical trials for alternative indications and subsequently became the first two antiviral agents to secure emergency use authorizations (EUAs) across numerous global jurisdictions. Interestingly,

while RDV secured regulatory approval as the pioneer direct-acting antiviral against SARS-CoV-2, the phase-3 clinical evaluation of FPV was terminated prematurely in March 2022 due to severe patient recruitment barriers caused by widespread global vaccination campaigns and the emergence of the Omicron variant, which presented clinically milder pathology than the preceding Delta variant¹.

A critical operational divergence exists in their modes of administration: RDV requires intermittent intravenous infusion, whereas FPV is administered orally, which dictates fundamental differences in their underlying pharmacokinetic profiles. Pharmacokinetics delineates the biological fate of an exogenous compound within a living system, encompassing its absorption, distribution, metabolism, and excretion (ADME) phases, whereas pharmacodynamics characterizes the systemic biochemical and physiological effects of the drug, governing its therapeutic efficacy and localized toxicity. To mimic these intricate biological kinetics and dynamics, machine-learning-driven ADMET analysis has emerged as a dominant computational methodology for predicting pharmacokinetic and toxicological endpoints. A significant portion of these predictive architectures is available as open-access, web-based platforms, where achieving an optimal ADMET profile serves as a core indicator of drug-like property configurations that balance safety and efficacy².

Although contemporary ADME prediction tools are primarily built upon the foundational physicochemical characteristics of small molecules, complementary toxicological platforms have integrated simulated human physiological parameters to refine projection outputs; nonetheless, a noticeable gap in precision persists when comparing *in silico* data against definitive clinical evidence. This predictive variance stems primarily from the dense anatomical and physiological complexity of human biological systems. The principal organs responsible for metabolic clearance and elimination in humans remain the liver, which drives enzymatic drug biotransformation, and the kidneys, which mediate the excretion of parent compounds and secondary metabolites³. Both the liver and kidneys possess highly specialized microstructures and functional pathways that must be thoroughly explored and integrated into computational ADMET matrices to enhance overall predictive precision. To the best of our knowledge, the present study represents the first modeling attempt to explicitly combine these unique human organ structures and physiological parameters within an advanced ADMET analysis framework. Consequently, this study aims to evaluate the predicted pharmacokinetic profiles and toxicological endpoints of RDV, FPV, and their respective metabolites by incorporating the unique anatomy and physiology of these primary elimination organs to generate highly precise and clinically relevant predictions.

MATERIALS AND METHODS

Materials

The Simplified Molecular Input Line Entry System (SMILES) strings for RDV, FPV, and their respective metabolites were retrieved directly from the open-access PubChem database (<https://pubchem.ncbi.nlm.nih.gov/>). These structural SMILES were subsequently used as input for systematic *in silico* profiling. The ADMET properties of the target antiviral compounds and their metabolic derivatives were comparatively evaluated using the web-based predictive platforms pkCSM (<https://biosig.unimelb.edu.au/pkcsm/prediction>), Deep PK (<https://biosig.lab.uq.edu.au/deeppk/prediction>), ProTox 3.0 (<https://tox.charite.de/protox3>), and ADMETLab 3.0 (<https://admetlab3.scbdd.com/server/evaluation>).

Methods

In silico ADMET protocol and canonical SMILES retrieval

The baseline pharmacokinetic and toxicological profiles of RDV, FPV, and their primary active metabolites were evaluated using open-access, web-based predictive platforms. SMILES identifiers for the parent drugs and their biotransformation products, comprising RDV monophosphate (RDV-MP), RDV triphosphate (RDV-TP), RDV parent nucleoside (RDV-N), and FPV riboside triphosphate (FPV-RTP), were retrieved from the PubChem database. These specific ASCII string-based line notations, which simplified the description of the chemical species structures, were systematically submitted to the pkCSM, ProTox 3.0, Deep PK, and ADMETLab 3.0 online servers to generate automated ADMET datasets⁴.

Organ-specific physiological adjustment protocol

To bridge the precision gap between automated simulations and human biology, the raw computational outputs from Deep PK were manually adjusted to account for the specific anatomy and physiology of the primary clearance organs. The automated metabolic and excretory prediction vectors were systematically modified by integrating localized human physiological parameters. These manual adjustments explicitly accounted for hepatic microstructures and biotransformation pathways alongside renal glomerular filtration and excretion mechanisms.

Data analysis

The physiologically adjusted ADMET datasets were compared with established clinical pharmacokinetic profiles and observed toxicological data from COVID-19 patient cohorts. This qualitative and quantitative correlation validated the predictive accuracy of the modified *in silico* model against real-world human clearance and toxicity outcomes.

RESULTS AND DISCUSSION

To achieve oral bioavailability, small-molecule candidates must satisfy Lipinski's Rule of Five (molecular weight under 500 Daltons, hydrogen bond acceptors up to 10, donors up to 5, and log P up to 5). Comparative structural analysis shows that FPV and the inactive clearance metabolite RDV-N meet these rules, indicating favorable intestinal permeability. Conversely, parent RDV, its phosphorylated forms (RDV-MP, RDV-TP), and the active FPV-RTP metabolite violate at least two parameters due to their excessive molecular weight or hydrogen-bonding capacity. Consequently, FPV is suitable for oral dosing, whereas RDV's low solubility and poor gastrointestinal absorption necessitate intravenous infusion. Structurally, the nucleotide analog prodrug RDV undergoes sequential intracellular phosphorylation to functional RDV-TP, while the pyrazine prodrug FPV undergoes intracellular phosphoribosylation to generate active FPV-RTP or is cleared into an inactive oxidative metabolite M1⁵⁶.

Predictive metrics across the pkCSM, ProTox 3.0, and ADMETLab 3.0 platforms (**Table I**) reveal that only parent FPV exhibits high intestinal absorption and the capacity to cross the blood-brain barrier (BBB), yielding a partition log BB value of 0.484. Within the cerebral vasculature, capillary endothelial cells form tight junctions that, alongside specialized receptors and efflux pumps, form the BBB to prevent unregulated entry into the central nervous system, restricting access primarily to small, lipid-soluble molecules with molecular weights between 400 and 600 Daltons. Following oral administration, FPV dissolves in gastric fluid and undergoes systemic absorption across the intestinal mucosal wall. While a minor fraction is cleared by intestinal motility or membrane-bound enzymes, the primary mass traverses the epithelial membrane to enter the portal vein system. Upon entering the liver via the hepatic portal vein, these molecules undergo extensive first-pass metabolism, removing a major fraction of the compound before it can enter the inferior vena cava and reach systemic circulation. This pre-systemic metabolism explains why most oral therapies exhibit an absolute bioavailability below 100%, indicating a clearance value (F) under 1⁷.

Pharmacokinetic predictions confirm that both RDV and FPV are extensively cleared via Phase 1 functional group modifications (oxidation, reduction, or hydrolysis) driven by cytochrome P450 enzymes and via Phase 2 conjugations that increase compound polarity. Specifically, FPV undergoes cytosolic hydroxylation mediated by aldehyde oxidase to yield its active antiviral forms, alongside minor xanthine oxidase clearance to produce the inactive M1 metabolite, before final excretion as a glucuronide conjugate⁶. Because aldehyde oxidase biotransformation occurs within the cytosol and completely avoids microsomal cytochrome P450 networks, FPV presents a significantly lower baseline risk for competitive drug-drug interactions than RDV.

Regarding clearance pathways, approximately 18% of administered RDV is eliminated via the feces, with the inactive RDV-N metabolite accounting for 0.5% of this fraction. *In silico* calculations demonstrate that parent RDV acts as a potent CYP2B6 inhibitor (p-value = 0.99), while the active metabolites RDV-TP and FPV-RTP serve as CYP2C9 substrates (p-value = 0.354), and parent FPV functions as a substrate for the highly inducible CYP1A2 isoenzyme (p-value = 0.874). Co-administration of CYP1A2-inducible agents such as omeprazole or primaquine increases the risk of competitive metabolic saturation due to shared transcriptional elements. Clinically, however, the primary metabolic interaction documented for FPV involves

only weak CYP2C8 inhibition⁸. This narrow interaction profile minimizes metabolic conflicts, suggesting that FPV may be a safer therapeutic alternative in intensive care settings where patients routinely receive complex polypharmacy regimens. Deep PK predictive metrics summarized in **Table II** indicate that FPV and FPV-RTP present a lower risk of causing type II drug-induced liver injury (DILI type II) than RDV derivatives, though parent FPV exhibits a higher likelihood of inducing type I injury, which reflects direct physiological events correlating with drug exposure. These modeling predictions correlate with randomized controlled trial data from moderate-to-severe COVID-19 cohorts, which documented abnormal liver function rates of 8% to 9% in FPV-treated arms compared with 3% to 6.5% in RDV-treated arms⁹.

Table I. The ADMET predictions of remdesivir, favipiravir, and their metabolites.

Compound	PubChem ID	MW	Volume	LogS	pKa (acid)	pKa (base)	Metabolism (DILI)(CYP)	Renal Clearance	$t_{1/2}$	Drug-induced nephrotoxicity	LD ₅₀ (mg/kg)	Skin Sensitization	Toxicity Class
Remdesivir (RDV)	121304016	602.23	571.087	-3.506	7.463	5.569	DILI (1.0) CYP2B6 inh (0.99)	3.023	4.564	0.953	1000	No (0.04)	4
Remdesivir monophosphate (RDV-MP)	121310009	371.06	310.963	-2.264	4.288	3.644	DILI (0.95)	0.295	10.99	0.997	1000	Possible (0.31)	4
Remdesivir triphosphate (RDV-TP)	56832906	531.02	403.359	-2.800	1.131	2.139	DILI (0.998) CYP2C9 sub (0.35)	-0.157	9.536	0.984	1000	Yes (0.99)	4
Remdesivir parent nucleoside (RDV-N)	44468216	291.26	267.650	-0.468	7.183	2.955	DILI (0.93)	1.315	10.365	0.417	1000	Possible (0.50)	4
Favipiravir (FPV)	492405	157.03	132.572	-0.715	8.384	1.794	DILI (0.90) CYP1A2 sub (0.874)	4.682	1.961	0.556	1190	No (0.06)	4
Favipiravir Riboside Triphosphate (FPV-RTP)	5271809	528.97	384.251	-2.969	1.038	3.316	DILI (0.996) CYP2C9 sub (0.817)	1.630	2.112	0.998	1190	No (0.99)	4

Table II. Deep PK elimination phase predictions of remdesivir, favipiravir, and their metabolites.

Compound	Excretion Half-Life Prediction	Excretion Half-Life Probability	Excretion Half-Life Interpretation	Excretion Clearance Log (mL/min/kg)	Excretion Clearance Interpretation	Toxicity Liver Injury I (DILI I)	Toxicity Liver Injury I Probability	Toxicity Liver Injury I Interpretation	Toxicity Liver Injury II (DILI II)	Toxicity Liver Injury II Probability	Toxicity Liver Injury II Interpretation
RDV	Half-life <3 hours	0.386	Low Confidence	4.28	Normal	Safe	0.243	Medium Confidence	Toxic	0.878	High Confidence
RDV-MP	Half-life ≥3 hours	0.660	High Confidence	5.11	Normal	Safe	0.206	Medium Confidence	Toxic	0.730	Medium Confidence
RDV-TP	Half-life <3 hours	0.386	Low Confidence	4.28	Normal	Safe	0.243	Medium Confidence	Toxic	0.878	High Confidence
FPV	Half-life <3 hours	0.386	Medium Confidence	9.07	Normal	Toxic	0.737	Medium Confidence	Toxic	0.610	Low Confidence
FPV-RTP	Half-life >3 hours	0.935	High Confidence	3.50	Normal	Safe	0.103	High Confidence	Toxic	0.512	Low Confidence

Both FPV and RDV rely on renal clearance as their primary systemic excretion route, a physiological process regulated by the structural perm-selectivity of the multi-layered glomerular filtration barrier. Located within the renal cortex, this barrier separates low-molecular-weight solutes from large plasma macromolecules using a negatively charged glycocalyx layer (50–300 nm), a fenestrated endothelial layer with 50–100 nm pores, an extracellular basement membrane, and highly differentiated epithelial podocytes. These podocytes form interdigitated filtration slits bridged by a 40-nm-wide slit

diaphragm composed of specialized adhesion proteins (nephrin, podocin, neph1, and fat1) that serve as the final size- and charge-selective filter. Because the active, phosphorylated metabolites of both therapies (RDV-MP, RDV-TP, and FPV-RTP) carry strong negative charges, they are electrostatically repelled by the negative charge of these slit diaphragms, shifting their primary elimination pathway toward hepato-biliary routes. In contrast, the uncharged parent drugs and their neutral nucleoside analogs are small enough to pass freely through the filtration slits, though the hydrostatic pressure driving this filtration generates continuous shear stress that leaves the glomerulus vulnerable to localized mechanical damage¹⁰.

Clinical clearance profiles indicate that RDV undergoes complex renal excretion, with 49% of the recovered dose eliminated via glomerular filtration as the inactive RDV-N metabolite and 10% cleared through active tubular secretion as the parent drug. Conversely, the renal clearance values for the polar intermediates RDV-MP and RDV-TP fall below 1.0 mL/min/kg, confirming their structural retention or subsequent clearance via hepato-biliary pathways. This hepatobiliary shift increases metabolic liver stress, which correlates with Deep PK models that classify RDV-TP as a high-confidence cause of type II liver injury¹¹. In contrast, FPV and its polar metabolites are cleared efficiently via glomerular filtration due to their low molecular weight and high water solubility, bypassing active tubular secretion mechanisms entirely. Consequently, the risk of inducing renal tubular impairment is significantly lower with FPV than with parent RDV, representing a distinct clinical advantage for FPV regimens in patients with compromised baseline kidney function⁶.

CONCLUSION

The integrated physiological-computational analysis demonstrates that FPV and its primary downstream metabolites exhibit a more favorable, drug-like ADMET profile than RDV and its corresponding chemical species in simulated human clearance systems. The predictive data indicate that FPV accommodates the intricate microstructures and metabolic pathways of the primary elimination organs with lower potential for localized toxicity and more predictable excretion kinetics. Based on these findings, it is highly recommended that subsequent computational pharmacology initiatives leverage advanced, artificial intelligence-driven ADMET platforms explicitly configured to mimic the complex anatomy and physiology of human organ functions.

ACKNOWLEDGMENT

The authors extend their sincere gratitude to the Dean of the Faculty of Pharmacy at Universitas Airlangga for providing the essential institutional facilities and administrative support that facilitated the successful execution of this research.

AUTHORS' CONTRIBUTION

Conceptualization: Anita Purnamayanti

Data curation: Anita Purnamayanti

Formal analysis: Anita Purnamayanti

Funding acquisition: -

Investigation: Anita Purnamayanti, Suharjono, Mahardian Rahmadi

Methodology: Anita Purnamayanti

Project administration: -

Resources: -

Software: -

Supervision: Suharjono, Mahardian Rahmadi

Validation: Suharjono, Mahardian Rahmadi

Visualization: -

Writing - original draft: Anita Purnamayanti

Writing - review & editing: Anita Purnamayanti, Suharjono, Mahardian Rahmadi

DATA AVAILABILITY

None.

CONFLICT OF INTEREST

The authors declared no conflict of interest related to this research.

REFERENCES

1. Vatsha P, Vardhan G, Kumari T, Kanwar N, Kanwal A, Deshmukh R. Efficacy and safety of remdesivir and favipiravir in COVID-19 patients - A systematic review and meta-analysis. *J Family Med Prim Care*. 2025;14(5):1604-16. DOI: [10.4103/jfmpc.jfmpc_1694_24](https://doi.org/10.4103/jfmpc.jfmpc_1694_24); PMID: [40547754](https://pubmed.ncbi.nlm.nih.gov/40547754/); PMCID: [PMC12178481](https://pubmed.ncbi.nlm.nih.gov/PMC12178481/).
2. Venkataraman M, Rao GC, Madavareddi JK, Maddi SR. Leveraging machine learning models in evaluating ADMET properties for drug discovery and development. *ADMET DMPK*. 2025;13(3):2772. DOI: [10.5599/admet.2772](https://doi.org/10.5599/admet.2772); PMID: [40585410](https://pubmed.ncbi.nlm.nih.gov/40585410/); PMCID: [PMC12205928](https://pubmed.ncbi.nlm.nih.gov/PMC12205928/).
3. Paliwal A, Jain S, Kumar S, Wal P, Khandai M, Khandige PS, et al. Predictive Modelling in pharmacokinetics: from in-silico simulations to personalized medicine. *Expert Opin Drug Metab Toxicol*. 2024;20(4):181-95. DOI: [10.1080/17425255.2024.2330666](https://doi.org/10.1080/17425255.2024.2330666); PMID: [38480460](https://pubmed.ncbi.nlm.nih.gov/38480460/).
4. Zhang S, Jeong S, Jiang B, Ho H. Pharmacokinetic simulations for remdesivir and its metabolites in healthy subjects and patients with renal impairment. *Front Pharmacol*. 2025;16:1488961. DOI: [10.3389/fphar.2025.1488961](https://doi.org/10.3389/fphar.2025.1488961); PMID: [40213698](https://pubmed.ncbi.nlm.nih.gov/40213698/); PMCID: [PMC11982744](https://pubmed.ncbi.nlm.nih.gov/PMC11982744/).
5. Schooley RT, Carlin AF, Beadle JR, Valiaeva N, Zhang XQ, Clark AE, et al. Rethinking Remdesivir: Synthesis, Antiviral Activity, and Pharmacokinetics of Oral Lipid Prodrugs. *Antimicrob Agents Chemother*. 2021;65(10):e0115521. DOI: [10.1128/AAC.01155-21](https://doi.org/10.1128/AAC.01155-21); PMID: [34310217](https://pubmed.ncbi.nlm.nih.gov/34310217/); PMCID: [PMC8448143](https://pubmed.ncbi.nlm.nih.gov/PMC8448143/).
6. Konstantinova ID, L Andronova V, Fateev IV, Esipov RS. Favipiravir and Its Structural Analogs: Antiviral Activity and Synthesis Methods. *Acta Naturae*. 2022;14(2):16-38. DOI: [10.32607/actanaturae.11652](https://doi.org/10.32607/actanaturae.11652); PMID: [35923566](https://pubmed.ncbi.nlm.nih.gov/35923566/); PMCID: [PMC9307979](https://pubmed.ncbi.nlm.nih.gov/PMC9307979/).
7. Azman M, Sabri AH, Anjani QK, Mustaffa MF, Hamid KA. Intestinal Absorption Study: Challenges and Absorption Enhancement Strategies in Improving Oral Drug Delivery. *Pharmaceuticals*. 2022;15(8):975. DOI: [10.3390/ph15080975](https://doi.org/10.3390/ph15080975); PMID: [36015123](https://pubmed.ncbi.nlm.nih.gov/36015123/); PMCID: [PMC9412385](https://pubmed.ncbi.nlm.nih.gov/PMC9412385/).
8. Lemaitre F, Solas C, Grégoire M, Lagarce L, Elens L, Polard E, et al. Potential drug-drug interactions associated with drugs currently proposed for COVID-19 treatment in patients receiving other treatments. *Fundam Clin Pharmacol*. 2020;34(5):530-47. DOI: [10.1111/fcp.12586](https://doi.org/10.1111/fcp.12586); PMID: [32603486](https://pubmed.ncbi.nlm.nih.gov/32603486/); PMCID: [PMC7361515](https://pubmed.ncbi.nlm.nih.gov/PMC7361515/).
9. Hassanipour S, Arab-Zozani M, Amani B, Heidarzad F, Fathalipour M, Martinez-de-Hoyo R. Addendum: The efficacy and safety of Favipiravir in treatment of COVID-19: a systematic review and meta-analysis of clinical trials. *Sci Rep*. 2022;12(1):1996. DOI: [10.1038/s41598-022-05835-2](https://doi.org/10.1038/s41598-022-05835-2); PMID: [35105913](https://pubmed.ncbi.nlm.nih.gov/35105913/); PMCID: [PMC8805134](https://pubmed.ncbi.nlm.nih.gov/PMC8805134/).
10. Daehn IS, Duffield JS. The glomerular filtration barrier: a structural target for novel kidney therapies. *Nat Rev Drug Discov*. 2021;20(10):770-88. DOI: [10.1038/s41573-021-00242-0](https://doi.org/10.1038/s41573-021-00242-0); PMID: [34262140](https://pubmed.ncbi.nlm.nih.gov/34262140/); PMCID: [PMC8278373](https://pubmed.ncbi.nlm.nih.gov/PMC8278373/).
11. Waldauf P, Jurisinova I, Svobodova E, Diblickova M, Tencer T, Zavora J, et al. The impact of remdesivir on renal and liver functions in severe COVID-19 patients with presence of viral load. *Sci Rep*. 2025;15(1):20900. DOI: [10.1038/s41598-025-05541-9](https://doi.org/10.1038/s41598-025-05541-9); PMID: [40594535](https://pubmed.ncbi.nlm.nih.gov/40594535/); PMCID: [PMC12214511](https://pubmed.ncbi.nlm.nih.gov/PMC12214511/).